

Inhibition of histone deacetylase activity induces developmental plasticity in oligodendrocyte precursor cells

Costas A. Lyssiotis*, John Walker[†], Chunlei Wu[†], Toru Kondo[‡], Peter G. Schultz*^{†§}, and Xu Wu^{†§}

*The Skaggs Institute of Chemical Biology and Department of Chemistry, The Scripps Research Institute, 10550 North Torrey Pines Road, La Jolla, CA 92037; [†]Genomics Institute of the Novartis Research Foundation, 10675 John Jay Hopkins Drive, San Diego, CA 92121; and [‡]Laboratory for Cell Lineage Modulation, RIKEN Center for Developmental Biology, 2-2-3 Minatojima-Minamimachi, Chuo-ku, Kobe 650-0047, Japan

Communicated by Kyriacos C. Nicolaou, The Scripps Research Institute, La Jolla, CA, August 1, 2007 (received for review June 12, 2007)

Recently, it was demonstrated that lineage-committed oligodendrocyte precursor cells (OPCs) can be converted to multipotent neural stem-like cells, capable of generating both neurons and glia after exposure to bone morphogenetic proteins. In an effort to understand and control the developmental plasticity of OPCs, we developed a high-throughput screen to identify novel chemical inducers of OPC reprogramming. Using this system, we discovered that inhibition of histone deacetylase (HDAC) activity in OPCs acts as a priming event in the induction of developmental plasticity, thereby expanding the differentiation potential to include the neuronal lineage. This conversion was found to be mediated, in part, through reactivation of *sox2* and was highly reproducible at the clonal level. Further, genome-wide expression analysis demonstrated that HDAC inhibitor treatment activated *sox2* and 12 other genes that identify or maintain the neural stem cell state while simultaneously silencing a large group of oligodendrocyte lineage-specific genes. This series of experiments demonstrates that global histone acetylation, induced by HDAC inhibition, can partially reverse the lineage restriction of OPCs, thereby inducing developmental plasticity.

cell-based screen | neural stem cells | Sox2

During mammalian development, stem cells become progressively restricted in the tissue types to which they can give rise, eventually differentiating into a single cell type. Classically, this process was considered irreversible. However, recent evidence suggests that differentiated cells can gain plasticity when transplanted into an embryonic environment (1) or, more strikingly, when a cell is forced to express unique gene combinations (2–4). Furthermore, in rare instances, progenitor cells can be induced by small molecules or growth factors to give rise to, what would otherwise be, restricted lineages (5, 6).

In the developing central nervous system, oligodendrocyte precursor cells arise from multipotent neural stem cells (NSCs) before they terminally differentiate into oligodendrocytes (OLs) (7). *In vitro*, oligodendrocyte precursor cells (OPCs) were believed to exist as bipotent and highly proliferative glial progenitor cells that can give rise to both OLs and type 2 astrocytes but were restricted from differentiating into neurons (8, 9). However, it was recently demonstrated that OPCs may have a wider developmental potential and can be converted to multipotent neural stem-like cells, capable of generating both neurons and glial cells after exposure to bone morphogenetic proteins (BMPs) (6). Analysis of this increase in developmental potential revealed transcriptional activation of NSC genes and silencing of OL lineage-specific genes that involved epigenetic modifications on histones (i.e., acetylation and methylation) and chromatin remodeling (10).

Clearly, there is considerable interest in understanding, as well as ultimately controlling, these complex processes for regenerative therapies. In particular, the identification of small molecules that induce reprogramming of mammalian cells would

provide further insights into the mechanisms that control cellular plasticity and may ultimately provide chemical reagents that make it possible to use healthy, abundant, and easily accessible adult cells to generate different types of stem/progenitor cells for therapeutic applications. Here, we identify a class of small molecules, histone deacetylase (HDAC) inhibitors, that, when used in conjunction with basic fibroblast growth factor (bFGF), are capable of reprogramming OPCs to a state of multipotency by global histone acetylation.

Results

High-Throughput Chemical Screening Strategy. To develop a high throughput screen to identify novel chemical inducers of OPC reprogramming (Fig. 1A), purified primary rat OPCs were transfected with a reporter construct that uses a 5.5-kb region of the *sox2* promoter to drive eGFP expression (P/Sox2-eGFP; Fig. 1A) (11). The SRY-related, HMG-box containing transcription factor Sox2 is expressed early in the developing neural tube and is essential for the maintenance of the multipotent state in NSCs (12). Additionally, Sox2 is highly expressed in NSCs but not in lineage restricted precursors, such as OPCs (10, 12, 13). Therefore, an increase in the multipotency of OPCs likely requires Sox2 expression, consistent with the previous observation that *sox2*-reactivation is essential for the BMP-2-induced conversion of OPCs to NSCs (10).

Treatment of the P/Sox2-eGFP OPC line (1,000 cells per well in a 384-well plate) with BMP-2 (20 ng/ml; $\approx 20\%$ GFP⁺) activated GFP expression in 25-fold more cells than did DMSO (<1% GFP⁺); BMP-2 was therefore used as a reliable and highly reproducible control in the small-molecule screen (Fig. 1B and C) (10). In-house combinatorial and known drug libraries ($\approx 40,000$ compounds at a final assay concentration of 2 μ M) were then screened to identify molecules that activate Sox2 expression in OPCs (13). Compounds that activated GFP expression at least 20-fold ($\approx 15\%$ GFP⁺) over DMSO control were identified as hits.

Because Sox2 reactivation alone may not be sufficient for OPC reprogramming, a secondary assay was developed to distinguish compounds that simply activate Sox2 from those that expand the differentiation potential of OPCs. OPCs are ordinarily restricted

Author contributions: C.A.L., P.G.S., and X.W. designed research; C.A.L. and J.W. performed research; T.K. contributed new reagents/analytic tools; C.A.L., C.W., P.G.S., and X.W. analyzed data; and C.A.L., P.G.S., and X.W. wrote the paper.

The authors declare no conflict of interest.

Abbreviations: AIC, astrocyte-inducing conditions; bFGF, basic fibroblast growth factor; BMP, bone morphogenetic protein; HDAC, histone deacetylase; NIC, neuron-inducing conditions; NSC, neural stem cells; OIC, oligodendrocyte-inducing conditions; OL, oligodendrocyte; OPC, oligodendrocyte precursor cell; RA, retinoic acid; TSA, trichostatin A.

[§]To whom correspondence may be addressed. E-mail: schultz@scripps.edu or xwu@gnf.org.

This article contains supporting information online at www.pnas.org/cgi/content/full/0707044104/DC1.

© 2007 by The National Academy of Sciences of the USA

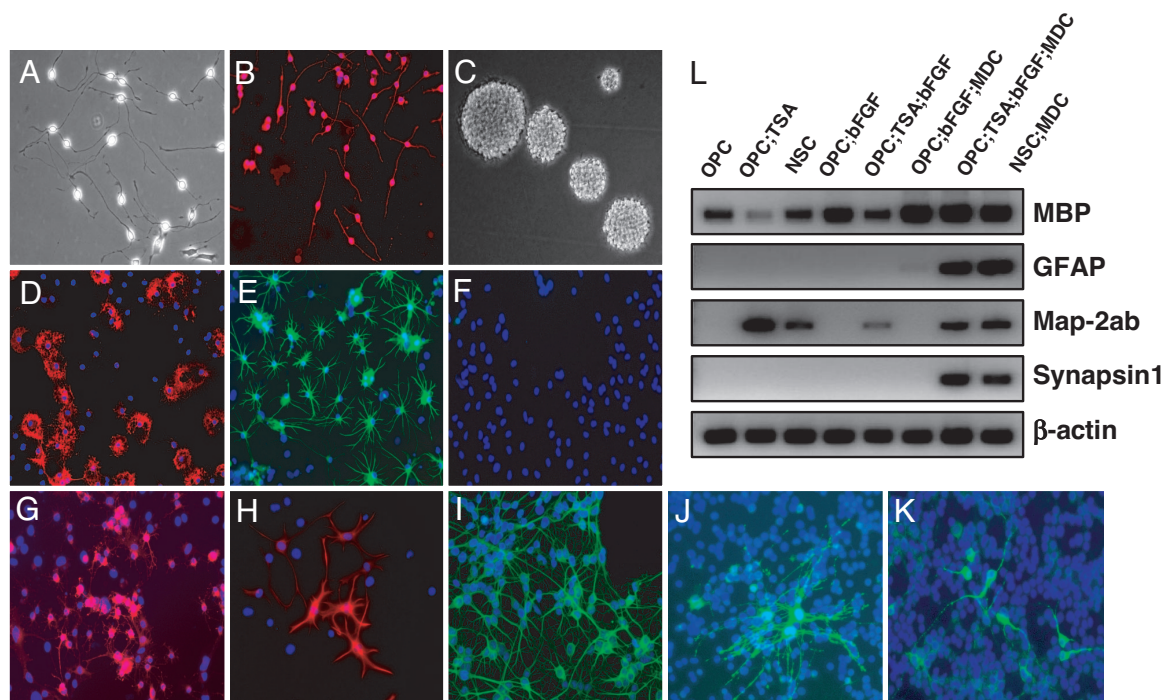


Fig. 3. Expression analysis of untreated and TSA-treated OPCs. (A and B) Perinatal OPCs maintain a bipolar morphology with phase bright cell bodies (A) and stain positive for A2B5 (B). (C) TSA-treated (20 nM) OPCs expanded as neuro/oligospheres in bFGF-containing NSC growth media. (D–F) Untreated OPCs express bipotent differentiation potential and stain positive for MBP under OIC (D) and GFAP under AIC (E) but do not display immunoreactivity for β III-tubulin when grown in NIC (F). (G–K) TSA-treated (20 nM) OPCs exhibit tripotent differentiation potential and stain positive for CNPase under OIC (G), GFAP under AIC (H), and a variety of neuronal markers under NIC, including β III-tubulin (I), NF-M (J), and Map-2ab (K). Nuclei are stained with DAPI and appear blue in all images. (L) Semiquantitative RT-PCR of neural gene expression. OPCs treated with TSA (20 nM), expanded in bFGF-containing media and exposed to mixed differentiation conditions [MDC; 1% FBS, 1 μ M retinoic acid (RA)] exhibited multipotent differentiation potential (lane 7) based on the expression of lineage-specific RNA transcripts for OLs (MBP), astrocytes (GFAP), and neurons (Map-2ab and Synapsin1). This expression profile was nearly indistinguishable from that of NSCs exposed to MDC (lane 8). Lane 1, untreated OPCs; lane 2, TSA-treated (20 nM) OPCs, 2 days; lane 3, untreated NSCs; lane 4, untreated OPCs expanded in NSC growth media, 7 days; lane 5, TSA-treated (20 nM, 2 days) OPCs expanded in NSC growth media, 7 days; lane 6, untreated OPCs expanded in NSC growth media and grown under MDC; lane 7, TSA-treated (20 nM, 2 days) OPCs expanded in NSC growth media and grown under MDC; lane 8, untreated NSCs grown under MDC.

Differentiation Potential. To identify the optimal cell culture parameters required for the induction of developmental plasticity in OPCs, a more thorough analysis was performed. OPCs are a well defined and characterized precursor cell type in the vertebrate CNS (22), and careful inspection of the OPC cultures before compound treatment confirmed their identity. The OPC cultures exhibited a homogenous bipolar morphology with phase bright cell bodies, consistent with a naive phenotype (Fig. 3A). Immunohistochemical examination confirmed that they expressed the perinatal OPC-specific antigen, A2B5, at >99% homogeneity (Fig. 3B). Additionally, the OPCs stained negative for more mature neural markers, including O4, galactocerebroside (GC), myelin basic protein (MBP), glial fibrillary acidic protein (GFAP), β III-tubulin, microtubule associate protein 2(a+b) (Map-2ab), and neurofilament-M (NF-M; data not shown). When OPCs were maintained in growth media in the absence (0.1% DMSO) of TSA for 2 days, expanded in sphere culture for 7 days and then maintained under NIC, astrocyte-inducing conditions (AIC), or OL-inducing conditions (OIC) (14), they exhibited bipotent differentiation potential, generating OLs (OIC) and astrocytes (AIC) but not neurons (Fig. 3D–F). Additionally, when OPCs were treated with TSA (20 nM) for 2 days and then subjected to lineage-specific differentiation conditions directly, they again only exhibited bipotent differentiation potential (data not shown). However, when OPCs were both treated with TSA 20 nM and then expanded in bFGF-supplemented NSC growth media in sphere culture, before lineage specific differentiation, they were capable of giving rise

to all three neural lineages (Fig. 3G–K). The expression of neuronal lineage-specific genes was confirmed both immunohistochemically and via semiquantitative RT-PCR. The OPC-derived neuronal cells expressed Map-2ab, NF-M, Synapsin1, and β III-tubulin at the protein and mRNA level (Fig. 3I–L).

Clonal Analysis. We then analyzed TSA-mediated OPC plasticity at the clonal level to rule out the possibility that the neurons observed in these experiments are derived from a residual NSC side population present after isolation of OPCs. Although it appeared that the primary OPC culture did contain a small population of cells with the potential to generate neurons (9 of 366 clones, \approx 2.5%), OPCs treated with 50 μ M NaBu (56 of 136 clones, 41%) or 20 nM TSA (41 of 129 clones, 32%) exhibited much higher potential to form neurons than the DMSO-treated control (SI Fig. 5). This experiment suggests that the HDAC inhibitor-mediated neuronal potential of OPCs does not result from the amplification of a residual multipotent side population of cells. NaBu was slightly more effective at reprogramming OPCs in this assay. However, NaBu is less specific than TSA and requires a significantly higher concentration (2,500-fold) to inhibit HDAC activity, whereas TSA, on the other hand, is a very potent and specific inhibitor (23). Therefore, we felt that TSA was a better tool to study HDAC inhibition and, as such, was used in the following analyses.

Microarray Analysis. Genome-wide transcription profiling was then used to further characterize the mechanism of HDAC inhibitor-

Table 1. Expression analysis of oligodendrocyte and neural stem/precursor-lineage markers

Gene	Function	Fold change in treated vs. untreated OPCs			
		6-h BMP-2	48-h BMP-2	6-h TSA	48-h TSA
Oligodendrocyte lineage					
<i>MBP</i>	Structural component of myelin	-12.9	-36.3	-20.4	-72.6
<i>MAG</i>	Structural component of myelin	-11.2	-51.3	-11.6	-52.6
<i>PLP</i>	Structural component of myelin	-5.7	-22.0	-5.8	-25.4
<i>OMG</i>	Inhibits proliferation and promotes OL differentiation	-1.6	-2.1	-34.2	-5.0
<i>CNPase</i>	Marker of myelin; associated with structural proteins	-2.9	-4.1	-4.1	-3.7
<i>Nkx2.2</i>	HD TF involved in OL differentiation	-5.8	-6.6	-32.5	-12.4
<i>Sox10</i>	HMG TF involved in OL differentiation	-2.3	-2.9	-9.7	-2.2
<i>Fyn</i>	Tyrosine kinase necessary for OPC maturation	-1.9	-2.5	-2.1	-2.1
Neural stem and progenitor					
<i>Nestin</i>	Structural protein expressed in CNS stem cells	3.4	2.4	5.2	6.1
<i>TenascinC</i>	Extracellular protein and neural precursor marker	1.0	1.1	16.7	34.2
<i>NeuroD1</i>	bHLH TF that promotes neurogenesis	1.0	0.9	2.6	2.3
<i>Foxg1</i>	Homeodomain-containing TF; regulates neurogenesis	3.0	2.7	2.1	2.4
<i>Id2</i>	HLH TF; maintains an immature, undifferentiated state	2.1	2.5	2.1	2.5
<i>Id4</i>	HLH TF; maintains an immature, undifferentiated state	2.8	6.3	2.5	2.8
<i>Smad5</i>	TF and downstream activator of BMP-signaling	4.8	5.7	7.0	2.9
<i>Sox9</i>	HMG TF; inhibitor of terminal glial differentiation	1.1	1.3	2.9	5.0
<i>Hey1</i>	bHLH TF activated by notch signaling	5.0	5.0	7.6	6.2
<i>Brcal</i>	TF involved in BMP-2-mediated reactivation of Sox2	8.8	11.8	9.3	9.3
<i>Hes1</i>	bHLH TF activated by notch; essential for neurogenesis	23.5	21.6	61.8	28.4
<i>Lhx2</i>	Homeodomain-containing TF; expressed in the developing CNS	59.5	68.2	105	114

mediated OPC plasticity and to compare this profile to that which results from BMP-2 induced OPC plasticity. OPCs were treated for 6, 12, 24, and 48 h with TSA (20 nM) or BMP-2 (20 ng/ml), and mRNA transcript profiles were compared with those of untreated cells by using the rat genome (230.2) array (Affymetrix, Santa Clara, CA). TSA treatment induced large-scale gene expression changes, displaying a >2-fold difference in 10,046 of the 30,000 probe sets at, at least, one time point. Of the 10,046 probe sets, 1,233 displayed a consistent pattern across all time points. Comparison of this set with that of the BMP-2-treated cells revealed a very high degree of similarity (SI Fig. 6), suggesting that TSA- and BMP-2-induced plasticity converge on a common transcriptional program.

The list of 1,233 probe sets was then sorted by function, which identified 145 genes (174 probe sets) involved in development (SI Table 2). Analysis of this sublist, with special regard to genes involved in OL differentiation (24), OPC self-renewal (25, 26), differentiation of NSCs to OPCs (27), OPC plasticity (10), or NSC self-renewal (11, 12, 28), revealed that eight of the most highly down-regulated genes upon treatment with TSA are associated with the differentiation of OPCs to OLs (Table 1). Interestingly, this group exhibited expression profiles nearly identical to those of BMP-2-treated OPCs and included proteins involved in myelin formation (*MBP*, *MAG*, *PLP*, *OMG*, and *CNPase*) (24) as well as other factors that promote the transition of OPCs to OLs (*Nkx2.2*, *Sox10*, and *Fyn*) (24, 29, 30). The data indicate that the down-regulation of OL-specific gene expression is a common feature of BMP-2- and HDAC-mediated OPC plasticity. More interestingly, 12 of the 145 genes are known to be involved in NSC self-renewal and are significantly up-regulated upon treatment with TSA (Table 1). This group includes the CNS stem cell markers *Nestin* and *Tenascin C* and a variety of transcription factors that mediate neural stem cell identity, including *NeuroD1*, *Foxg1*, *Id2*, *Id4*, *Smad5*, *Sox9*, *Hey1*, *Brcal*, *Hes1*, and *Lhx2* (10, 30–33). The expression profiles of these 12 genes also exhibit a high degree of similarity in BMP-2- and TSA-treated OPCs. In light of the above experiments, it appears that the two mechanisms of OPC-plasticity

may involve similar changes in gene expression patterns during the conversion to a multipotent state.

Discussion

Development and cell fate determination require genetic and epigenetic coordination. For instance, as a naïve cell differentiates toward a particular lineage, modifications of the chromatin occur that activate lineage-specific genes and silence “stemness” genes and those associated with alternative cell fates (34). Although it was thought that this was an irreversible process, recent evidence presented here and elsewhere has refuted that dogma. The most striking example comes from the lab of Shinya Yamanaka (2), who demonstrated that ectopic expression of Oct-4, Sox2, Klf4 and c-Myc can convert terminally differentiated skin cells into pluripotent embryonic stem cells. Work done in our lab by Chen *et al.* (5, 35) has also made a significant contribution to this notion, demonstrating that a small molecule, reversine, can expand the differentiation potential of lineage restricted myoblasts to include the osteoblast and adipocyte lineages by modulating the activity of nonmuscle myosin II heavy chain and MEK1. Here, we further demonstrate that global histone acetylation, induced by HDAC inhibition, can partially reverse the lineage restriction of OPCs, thereby inducing developmental plasticity. Indeed, OPCs rapidly acquire several molecular characteristics of NSCs when treated with TSA, including activation of 13 genes that identify or maintain the neural stem cell state while simultaneously silencing a large group of OL lineage-specific genes (Table 1).

One of the changes that we suspect is required for OPC plasticity is the reactivation of *sox2*. Although *sox2* is not expressed in OPCs, it is expressed in TSA-treated OPCs and in NSCs, which are thought to give rise to OPCs (7). Indeed, ChIP analysis showed that the R1 region of the *sox2* promoter is modified to a partially open state in response to TSA and fully activated when TSA-treated cells are expanded in bFGF (Fig. 2). The ChIP data are consistent with the observation that TSA-treated OPCs (demonstrating partial *sox2* activation) submitted directly to NIC, without bFGF expansion, do not exhibit mul-

tipotent differentiation potential, whereas those that are bFGF-expanded (demonstrating full *sox2* activation) are tripotent. Therefore, *sox2* expression, driven by the state of the chromatin at its promoter (“partially activated” vs. “fully activated”) likely plays a central role in OPC reprogramming. Moreover, inhibition of TSA-induced Sox2 reexpression significantly reduced neurogenesis in TSA-treated OPCs, indicating that Sox2 is a critical component for establishing the multipotent neural stem cell-like state (SI Fig. 4). This is consistent with previous work demonstrating that Sox2 activity is required for BMP-2-induced OPC plasticity (10). There is a heterogeneity in the reprogramming response to TSA treatment ($\approx 35\%$ of cells express Sox2; Fig. 1D), which was also observed in morphogen-induced plasticity ($\approx 20\%$ of cells are Sox2-positive in response to BMP-2 treatment). This suggests that other factors may be involved, such as stage of the cell cycle, which was shown to play a role in the activity of reversine (35).

The identification of BMP-2 induced genes in HDAC-treated OPCs is in good agreement with previous studies on OPC plasticity. In particular, *Smad5* and the *Id* genes are specific downstream transcriptional regulators of BMP-signaling (33), and their induction upon HDAC treatment provides strong evidence for cross-talk between these two processes. In addition, *Hes1* and *Bra1* were previously implicated in BMP-2-induced OPC plasticity, and *Bra1*, in particular, was found to be associated with the chromatin remodeling complex involved in the reactivation of Sox2 (10). However, although the expression profiles of BMP-2- and TSA-treated cells look quite similar, and many BMP-signature genes are up-regulated in response to TSA, the BMP pathway is not directly operative in HDAC-mediated OPC plasticity. For instance, BMP-2 expression was not identified in the microarray analysis for TSA-treated or untreated OPCs. Moreover, when TSA-treated OPCs are grown in the presence of Noggin, a BMP antagonist, a robust reprogramming response is still observed (data not shown). Lastly, TSA-treated cells do not express GFAP, and thus HDAC-induced OPC plasticity does not require conversion to type-2 astrocytes, a critical requirement in BMP-induced OPC plasticity (10).

In summary, we discovered that inhibition of HDAC activity in OPCs acts as a priming event in the induction of developmental plasticity, thereby expanding the differentiation potential to include the neuronal lineage. This conversion was found to be mediated, in part, through reactivation of *sox2* and was highly reproducible at the clonal level. Further, genome-wide expression analysis demonstrated that HDAC treatment activated a series of genes that identify or maintain the neural stem cell state while simultaneously silencing a large group of oligodendrocyte lineage-specific genes. Finally, future work will focus on examining the activity of HDAC inhibition in other cell systems and on determining the precise combination of factors that afford OPCs multipotent differentiation potential. Ultimately such studies may lead to small molecules for the study and therapeutic use of stem cell potential.

Materials and Methods

Chemicals. All chemicals were purchased from Sigma (St. Louis, MO), with the exception of Apicidin (Alexis, Lausen, Switzerland). The design of in-house combinatorial small-molecule libraries has been described (13).

Cell Culture. P6 rat optic nerve OPCs were purified to $>98\%$ purity by sequential immunopanning as described (36) and cultured on poly-D-lysine ($10 \mu\text{g/ml}$)-coated flasks in B27- (without vitamin A; Invitrogen, Carlsbad, CA) supplemented DMEM/F12 (Invitrogen) containing PDGF-AA (10 ng/ml ; Peprotech, Rocky Hill, NJ) at 37°C with $8\% \text{ CO}_2$. OPCs were used between passage 5 and 20 and were never allowed to reach confluence to maintain the naïve state.

Rat hippocampal NSCs, a generous gift from the laboratory of Fred Gage (The Salk Institute, La Jolla, CA), were cultured on poly-D-lysine (PDL, $10 \mu\text{g/ml}$) and laminin ($10 \mu\text{g/ml}$; Invitrogen)-coated 75-cm^2 tissue culture flasks in N2 (Invitrogen) supplemented DMEM/F12 containing bFGF (20 ng/ml ; Invitrogen).

Transfection, Reporter Assay, and Compound Screens. The P/Sox2-eGFP construct, another generous gift from Fred Gage, was cotransfected with a plasmid conferring neomycin resistance at a 20:1 ratio with FuGENE6 (Roche, Indianapolis, IN), according to the manufacturer's instructions. After 2 days, $400 \mu\text{g/ml}$ G418 (Invitrogen) was added to growth media to generate a stable line. The P/Sox2-eGFP line was then plated at single-cell density on 96-well PDL-coated plates. Individual clones that demonstrated high GFP expression in the presence of BMP-2 (20 ng/ml ; Peprotech) and low background fluorescence in the absence of stimulation were then used in high-throughput chemical screens. For screening, P/Sox2-eGFP OPCs were plated at a density of 1,000 cells/well on PDL-coated 384-well plates (Greiner, Philadelphia, PA) in growth media. Compounds were added at a final concentration of $2 \mu\text{M}$ 12 h after plating. Cells were treated with compounds for 2.5 days and fixed for 20 min with a 10% formalin solution, after which cell nuclei were stained with DAPI.

High-Content Imaging. Fixed and stained plates were imaged by using the Opera confocal imaging reader and analyzed with the Opera software (Evotec Technologies, Boston, MA). An air $\times 10$ lens was used to capture six images at both wavelengths (460 and 535 nm), representing different locations in a single well. For image analysis, DAPI-stained nuclei and GFP-positive cell bodies were detected by using an algorithm that selects for positive cell bodies and nuclei within a range of fluorescent emission values and sizes (SI Fig. 7), as determined by fitting parameters to positive (BMP-2, 20 ng/ml) and negative controls (DMSO, 0.1%). Numerical results from the analyzed images were later exported for analysis in Excel (Microsoft, Redmond, WA).

ChIP Assay. ChIP assays using 3×10^6 cells per reaction were performed according to the manufacturer's recommendation (catalog no. 17-245; Upstate Biotechnology; Lake Placid, NY). The following antibodies were used for the assay: anti-dimethyl-histone H3-K4 ($10 \mu\text{g}$; Upstate Biotechnology), anti-dimethyl-histone H3-K9 ($10 \mu\text{g}$; Upstate Biotechnology), anti-acetyl-histone H3-K9 ($10 \mu\text{g}$; Upstate Biotechnology), and anti-FLAG ($10 \mu\text{g}$; Sigma). Primer sets for the R1 locus of the *sox2* promoter were described (10). Cycle parameters were 10 sec at 94°C , 20 sec at 60°C , and 90 sec at 72°C for 30 cycles.

Differentiation Conditions and Clonal Analysis. OPCs maintained in growth medium were treated with compound for 2 days, trypsinized (0.05% ; Invitrogen), and replated on ultralow-adhesion dishes (ULA; Corning, Corning, NY) in NSC growth medium for 7 days to expand the reprogrammed NSLC population. Neurospheres were collected by centrifugation, trypsinized, and plated on PDL and laminin-coated 96-well plates for 2–3 days in NSC growth medium. bFGF was then withdrawn from NSC growth medium, and the NSLC population was directed toward the various neural lineages via medium supplementation with the following factors; oligodendrocyte (OIC); insulin growth factor (IGF1, 500 ng/ml ; R & D Systems, Minneapolis, MN) and 100 nM T_3 ; Astrocyte (AIC), leukemia inhibitory factor (LIF, 50 ng/ml ; Chemicon, Temecula, CA), and 50 ng/ml BMP-2; Neuron (NIC), $1 \mu\text{M}$ RA and $5 \mu\text{M}$ forskolin. To generate a heterogeneous population of the neural lineages, NSC growth medium was supplemented with 1% FBS and $1 \mu\text{M}$ RA. Differentiation was assessed at 4, 7, and 10 days, depending on the stage-specific presentation of the marker in question.

OPC clones were generated by plating cells at ≈ 1 cell per well

in OPC growth medium on PDL-coated 96-well plates. Clones were expanded for 2 weeks with half of the medium replaced every 3 days. After 2 weeks, fresh OPC growth medium was added containing 50 μ M NaBu, 20 nM TSA, or 0.1% DMSO. Clones were treated for 2 days, trypsinized, and replated on uncoated 96-well plates in NSC growth medium and expanded for 7 days. The clones were then transferred to 96-well PDL- and laminin-coated plates, primed, and directed toward the neuronal lineage for an additional 7 days, after which they were fixed and stained for neuron-specific type III β -tubulin. Reprogrammed clones were identified by expression of β III-tubulin in >1% of the cells.

The NSC control samples were plated at \approx 1 cell per well in 96-well PDL- and laminin-coated plates, expanded in growth media for 2 weeks, primed, and directed toward the neuronal lineage via bFGF removal and supplementation of RA and forskolin.

Immunocytochemistry and Antibodies. Immunostaining was carried out by using standard protocols. Primary antibodies and dilutions are provided in [SI Table 3](#). Secondary antibodies were Cy2- or Cy3-conjugated anti-rabbit or anti-mouse (1:500; Jackson ImmunoResearch, West Grove, PA). Nuclei were counterstained with DAPI. Cells were imaged by using a Eclipse TE2000-U microscope (Nikon, East Rutherford, NJ) with \times 100 or \times 200 magnification. Double-label images were assembled in METAMORPH.

Semiquantitative RT-PCR Analysis. Total RNA from different samples was isolated and purified by using the RNeasy Mini kit with on-column DNase digestion (Qiagen, Valencia, CA). Single-stranded cDNA was synthesized from 5 μ g of total RNA with the SuperScript III First-Strand Synthesis System for RT-PCR using oligo(dT)₂₀ primers (Invitrogen). PCRs were run by using the Expand High Fidelity polymerase (Roche) and gene-specific primers ([SI Table 4](#)). Cycle parameters for all genes were 30 s at 94°C, 60 s at 57°C, and 60 s at 72°C for 25 cycles. The amount of total RNA and PCR conditions were optimized so that amplification of both β -actin and the cDNAs of interest were in the exponential phase.

GeneChip Hybridization. Sample preparation for GeneChip analysis was carried out according to the protocol detailed by Affymetrix. Briefly, first- and second-strand cDNAs were synthesized, double-stranded cDNA was *in vitro* transcribed by using the Affymetrix 3' amplification kit, and the resulting cRNA was purified, fragmented, and hybridized to oligonucleotide arrays (Rat Genome 230 2.0 Array, catalog no. 900507; Affymetrix). Arrays were processed by using standard Affymetrix protocols. The Affymetrix Hybridization Control kit and PolyA RNA control kit were used for the hybridizations.

Microarray Data Analysis. Probe values from CEL files were condensed to probe sets by using the gcRMA package from Bioconductor (www.bioconductor.org) and the R program (R Foundation for Statistical Computing, ISBN 3-900051-07-0). The gene expression levels from microarray experiments were quantified by gcRMA with quantile-normalization. Data were unlogged and median scaled to a value of 100. We then filtered out those absent or unchanged genes by requiring expression across samples greater than a value of 200 in at least one experimental group (twice the median across the array) and the fold change across samples at least 2-fold (ratio of maximum/minimum expression across all experimental groups). Probe sets met the aforementioned criteria and were left after filtering. Functional annotation of a selected set of genes was performed in DAVID Tools (<http://david.abcc.ncifcrf.gov>). Enrichment scores were based on the 10,046 background probe sets identified after filtering.

Note Added in Proof. Liu *et al.* (37) published work supporting our findings while this manuscript was out for review, in which OPCs isolated from rat cortex and treated with HDAC inhibitors were able to engraft and form functional neurons *in vivo*.

We thank Dr. Fred Gage for providing the P/Sox2-eGFP construct and rat hippocampal NSCs; Drs. Charles Cho and Daniel Rines for imaging-based HTS; Stephen Ho for his assistance with the microarray; and Drs. Shoutian Zhu, Jun Liu, Andrew Su, and Sheng Ding for helpful discussions. This work is supported by a National Science Foundation Predoctoral Fellowship (C.A.L.), the Skaggs Institute of Chemical Biology of The Scripps Research Institute (P.G.S.), and the Novartis Research Foundation (P.G.S. and X.W.). This is manuscript number 18908 of the Scripps Research Institute.

- Eggen K, Baldwin K, Tackett M, Osborne J, Gogos J, Chess A, Axel R, Jaenisch R (2004) *Nature* 428:44–49.
- Takahashi K, Yamanaka S (2006) *Cell* 126:663–676.
- Watanabe Y, Kameoka S, Gopalakrishnan V, Aldape KD, Pan ZZ, Lang FF, Majumder S (2004) *Genes Dev* 18:889–900.
- Xie H, Ye M, Feng R, Graf T (2004) *Cell* 117:663–676.
- Chen S, Zhang Q, Wu X, Schultz PG, Ding S (2004) *J Am Chem Soc* 126:410–411.
- Kondo T, Raff M (2000) *Science* 289:1754–1757.
- Gage FH (2000) *Science* 287:1433–1438.
- Barres BA, Lazar MA, Raff MC (1994) *Development (Cambridge, UK)* 120:1097–1108.
- Mabie PC, Mehler MF, Marmur R, Papavasiliou A, Song Q, Kessler JA (1997) *J Neurosci* 17:4112–4120.
- Kondo T, Raff M (2004) *Genes Dev* 18:2963–2972.
- D'Amour KA, Gage FH (2003) *Proc Natl Acad Sci USA* 100 Suppl 1:11866–11872.
- Graham V, Khudyakov J, Ellis P, Pevny L (2003) *Neuron* 39:749–765.
- Ding S, Gray NS, Wu X, Ding Q, Schultz PG (2002) *J Am Chem Soc* 124:1594–1596.
- Hsieh J, Nakashima K, Kuwabara T, Mejia E, Gage FH (2004) *Proc Natl Acad Sci USA* 101:16659–16664.
- Kubota A, Nishida K, Nakashima K, Tano Y (2006) *Biochem Biophys Res Commun* 351:514–520.
- Shen S, Li J, Casaccia-Bonnel P (2005) *J Cell Biol* 169:577–589.
- Liu A, Muggironi M, Marin-Husstege M, Casaccia-Bonnel P (2003) *Glia* 44:264–274.
- Bernstein BE, Meissner A, Lander ES (2007) *Cell* 128:669–681.
- Kouzarides T (2007) *Cell* 128:693–705.
- Klose RJ, Zhang Y (2007) *Nat Rev* 8:307–318.
- Yamanaka S (2007) *Stem Cell* 1:39–49.
- Barres BA, Raff MC (1994) *Neuron* 12:935–942.
- Johnstone RW (2002) *Nat Rev Drug Discov* 1:287–299.
- Gokhan S, Marin-Husstege M, Yung SY, Fontanez D, Casaccia-Bonnel P, Mehler MF (2005) *J Neurosci* 25:8311–8321.
- Kondo T, Raff M (2000) *Development (Cambridge, UK)* 127:2989–2998.
- Kondo T, Raff M (2000) *EMBO J* 19:1998–2007.
- Hu JG, Fu SL, Zhang KH, Li Y, Yin L, Lu PH, Xu XM (2004) *J Neurosci Res* 78:637–646.
- Bylund M, Andersson E, Novitsch BG, Muhr J (2003) *Nat Neurosci* 6:1162–1168.
- Sperber BR, Boyle-Walsh EA, Engleka MJ, Gadue P, Peterson AC, Stein PL, Scherer SS, McMorris FA (2001) *J Neurosci* 21:2039–2047.
- Wegner M, Stolt CC (2005) *Trends Neurosci* 28:583–588.
- Hanashima C, Li SC, Shen L, Lai E, Fishell G (2004) *Science* 303:56–59.
- Porter FD, Drago J, Xu Y, Cheema SS, Wassif C, Huang SP, Lee E, Grinberg A, Massalas JS, Bodine D, *et al.* (1997) *Development (Cambridge, UK)* 124:2935–2944.
- Ying QL, Nichols J, Chambers I, Smith A (2003) *Cell* 115:281–292.
- Meshorer E, Misteli T (2006) *Nat Rev* 7:540–546.
- Chen S, Takanashi S, Zhang Q, Xiong W, Peters EC, Ding S, Schultz PG (2007) *Proc Natl Acad Sci USA* 104:10482–10487.
- Barres BA, Hart IK, Coles HS, Burne JF, Voyvodic JT, Richardson WD, Raff MC (1992) *Cell* 70:31–46.
- Liu A, Han YR, Li J, Sun D, Ouyang M, Plummer MR, Casaccia-Bonnel P (2007) *J Neurosci* 27:7339–7343.